Supporting Information

FDM 3D printing of high pressure, heat resistant, transparent microfluidic devices

Valentin Romanov[#,1], Raheel Samuel[#,1,2], Marzieh Chaharlang[1], Alexander R. Jafek[1], Adam Frost[3,4,5,6], Bruce K.Gale[1],

Affiliations

[1]Department of Mechanical Engineering, University of Utah, Salt Lake City, UT, 84112 USA

[2]Department of Surgery, University of Utah, Salt Lake City, UT, 84112 USA

[3]Department of Biochemistry, University of Utah, Salt Lake City, UT, 84112 USA

[4]Department of Biochemistry and Biophysics, University of California, San Francisco, San Francisco, CA 94158 Sax1

[5]California Institute for Quantitative Biomedical Research, San Francisco, CA 94158 USA

[6]Chan Zuckerberg Biohub, San Francisco, CA 94158 USA

# These authors contributed equally to this work

Corresponding author (email)

bruce.gale@utah.edu

Abstract
In order to expedite replication of the results found in the main article printing parameters and a troubleshooting guide is provided. Further detail is provided on the nature of the transparency, contrasting against published transparent microfluidic devices. Detailed graphics and methods are provided for fabrication of annealed microfluidic devices along with information on the testing rig utilized for DNA melting.

Contents

Methods

Pressure characterization

High pressure tubing was attached to a 1600 PSI pressure transducer (MK-1600) with one end fixed to a high-pressure pump (LC-10AD, Shimadzu). The outlet line from the pressure transducer was attached to the device via high pressure fittings. Pressure drop across the transducer was measured via an in-house LabView program. A constant flow rate of 0.1 ml/hr was applied at the pump. With only an inlet, pressure was monitored until device failure.

Mixing and transparency characterization

Mixing was quantified using the following formula:

$$\boldsymbol{Average\ standard\ deviation\ at\ a\ specific\ turn} = \frac{\boldsymbol{\sigma_{R+}\sigma_{G+}\sigma_{B}}}{\boldsymbol{3}} = \boldsymbol{\sigma_{ave}}\ \#(\mathbf{1})$$

$$\sigma_N = \frac{\sigma_{ave}}{ave.standard\ deviation\ of\ unmixed\ streams}\ \#(2)$$

where $\boldsymbol{\sigma_R}, \boldsymbol{\sigma_G}, \boldsymbol{\sigma_B}$ is the standard deviation of the red, green and blue channels, respectively.

For quantifying transparency with increasing channel depth, each channel (RGB) was quantified in ImageJ, and normalized to glass using the following formula:

$$\sigma_1 = normalization = \left[\frac{\sigma_{R+}\sigma_{G+}\sigma_B}{3}\right] \times \frac{1}{\sigma_{Glass,max}}\ \#(3)$$

where σ_1 is the ratio of material, turn specific average standard deviation to that of glass, $\sigma_2$is used to scale this ratio to that off glass, where σ_{Glass} is the average standard deviation of the RGB channels taken from a glass-integrated 3D printed device.

Device annealing

Several devices consisting of a 100 µm thick visualization layer and a 400 x 400 µm channel were printed in Crystal Clear PLA. Overall device thickness was 700 µm. Each device was measured before and after annealing. Channel deformation was measured with callipers and a light microscope. Devices were measured in width, height and thickness. Channels cross sections were measured in ImageJ. Devices were annealed on a hotplate at either 100, 120 or 140 °C for 10 minutes. To prevent initial warping, double sided tape was placed onto a thin metal surface underneath the PLA devices. The metal plate was then placed onto a hotplate. Heat resistance was measured by placing annealed devices without any supporting structure (as-is) back onto the hotplate (95 °C for 5 min) and comparing deformation to un-annealed devices.

Imbedded channel

A 400 μm channel was imbedded 400 μm into the device. The print was carried out by following the procedures outlined in this paper with a few modifications. First, to ensure consistent channel formation the length of the channel should be facing directly towards the cooling fan. Having the main channel perpendicular to the cooling fan leads to closed and inconsistent channels. Second, we found it was necessary to slightly alter the code to prevent blockage of the channels at the point of constriction (where water meets oil). To do this, we modified a single layer within the GCODE to extrude half of the original amount of filament for a single layer.

Supplementary Figures

CRITICAL PRINTING PARAMETERS					
Material	**First Layer Temp (ºC)**	**Nozzle Temp (max)(ºC)**	**Bed Temp (max)(ºC)**	**Perimeter speed (max) (mm/s)**	**Extrusion multiplier**
PETg-XT	270	254	70-80	50	0.94
CC-PLA	210	200	50-55	33	1
In-PLA	220	210	70	33	1
PETg t-Glase	240	237	70	10	1
Nylon 680	247	245	40	20	0.81

COMMENTS AND OBSERVATIONS		
Material	**Rating**	**Comments**
PETg XT	+	Very strong adhesion to print surface
	+	Strong
	+	Flexible
	-	Requires optimization
	-	Requires high temperatures
	-	Will ooze at temperatures above 270 C
PETg t-Glase	+	Very strong parts
	+	Highly transparent
	+	Good surface adhesion
	+	Flexible
	-	Very slow print speeds
	-	Requires a lot of optimization
In-PLA	+	Easy to print
	-	Extremely brittle
	-	Very poor adhesion to glass
	-	Poor interlayer adhesion
Crystal Clear PLA	+	Very easy to print
	+	Easy to bridge channels
	+	Good surface adhesion
	-	Rigid
Nylon 680	+	Good surface adhesion
	+	Can be autoclaved
	+	High heat resistance
	+	Very flexible
	-	Oozing can be a problem
	-	Requires a lot of optimization
	-	Relatively slow print speeds
	-	Very poor layer adhesion below 240 C

Figure S1. Printing parameters. Printing parameters for each material with associated comments. This table should act as a quick-start guide.

	POTENTIAL PROBLEM	POTENTIAL SOLUTIONS
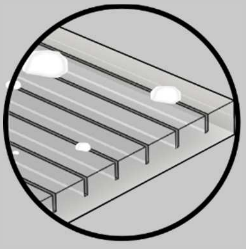	White zits	Adjust z-height
	Stringing	Lower nozzle temperature
	Smearing of deposited layer	Lower bed temperature
		Adjust retraction speed and length
		Check travel distance
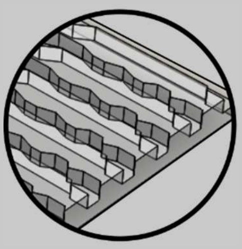	Irregular filament deposition	Increase extrusion multiplier
	Filament not extruding in a continuous line	Increase nozzle temperature
		Ensure filament spool is turning freely
		Ensure the z-height is properly calibrated
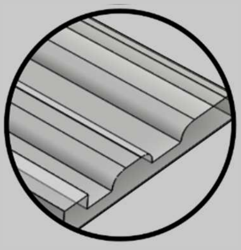	Channel width and or height is incorrect	Lower nozzle temperature
	Channel tapering	Lower bed temperature
		Incorrect z-height
		Increase cooling rate
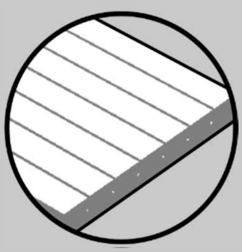	Poor transparency	Increase nozzle temperature
		Adjust z-height (closer to bed)
		Lower print speed
		Increase extrusion multiplier
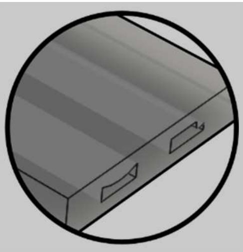	Poor bridging	Reduce bridging flow rate
	Channels filling	Reduce nozzle temperature
	Channel buckling	Increase print speed
		Modify bridging angle
		Align print to cooling fan
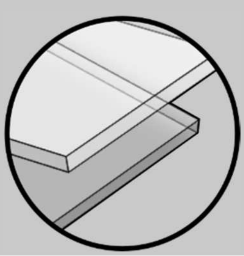	Poor adhesion to glass	Increase nozzle temperature
	Filament delaminating	Increase bed temperature
		Lower nozzle closer to surface
		Clean surface with alcohol
		Turn fan off for first layer

Figure S2. Troubleshooting guide. A highlight of the most common problems encountered during fabrication of microfluidic devices.

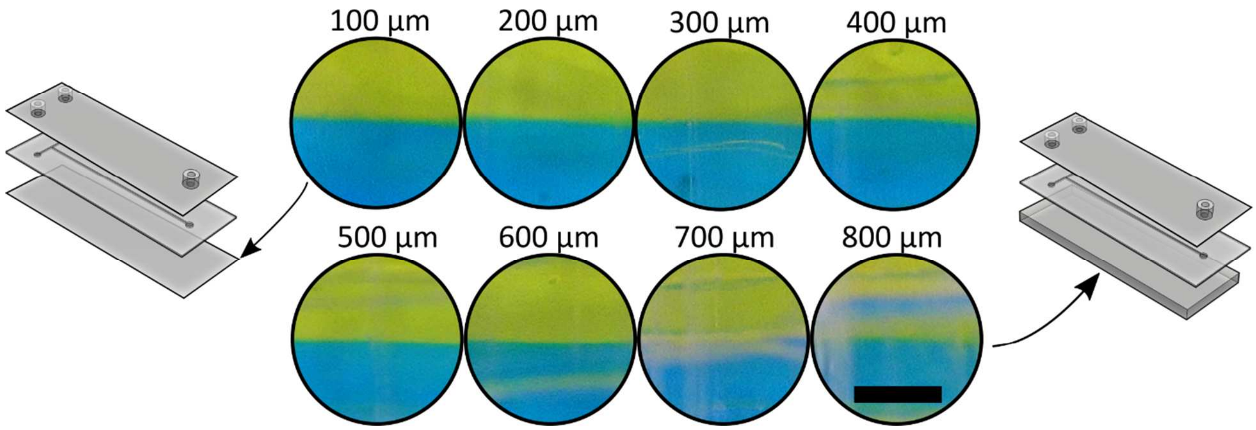

Figure S3. Thicker gL2 layer. While a single 100 um layer is practically as transparent as glass, the transparency decreases with increased layer deposition. With an 700 um gL^2, discerning the two-dye interface becomes much harder. Material; Crystal Clear PLA. Scale bar, 0.25 mm.

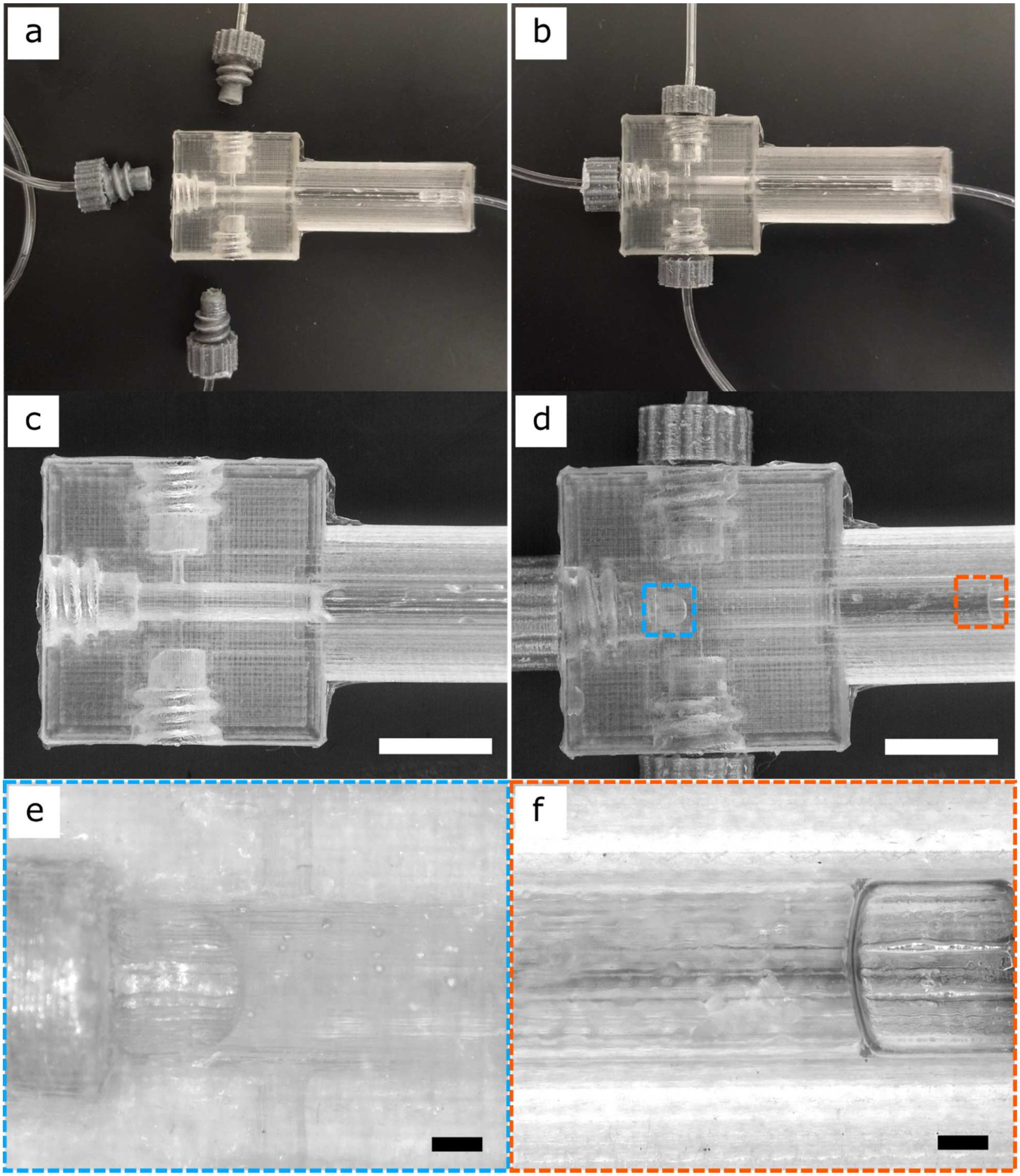

Figure S4. Inner and outer threading. a, A simple co-flow junction 3D printed using the parameters described (included in .ini file) for CC PLA. The device is not filled, i.e. just air inside the device. b, With threads screwed in. c, Close up of a. Channels are imbedded 500 µm into the device. Scale bar, 10 mm. d, Device is filled with water. Scale bar, 10 mm. e, Close up of an air droplet inside the microfluidic device. Smaller air droplets are also visible. Scale bar, 1 mm. f, Close of the main channel showing the highly transparent interface between air and water. Scale bar, 1 mm.

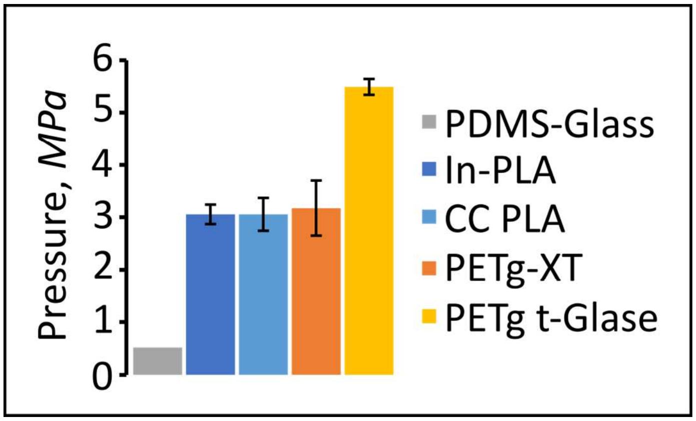

Figure S5. Max pressure before device failure. A 400 x 400 µm channel is printed on top of a single 3D printed layer (100 µm thick) to quantify maximum pressure at best possible transparency (n=4).

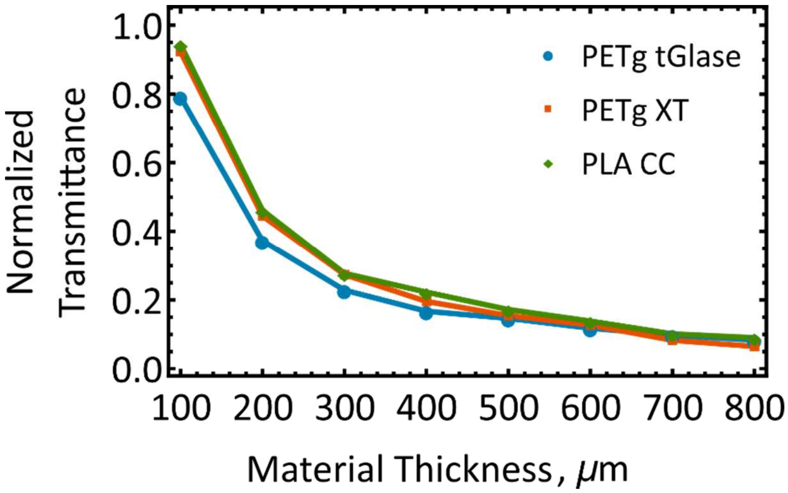

Figure S6. Transmittance normalized to glass, based on material thickness. Change in transmittance with increasing material thickness.

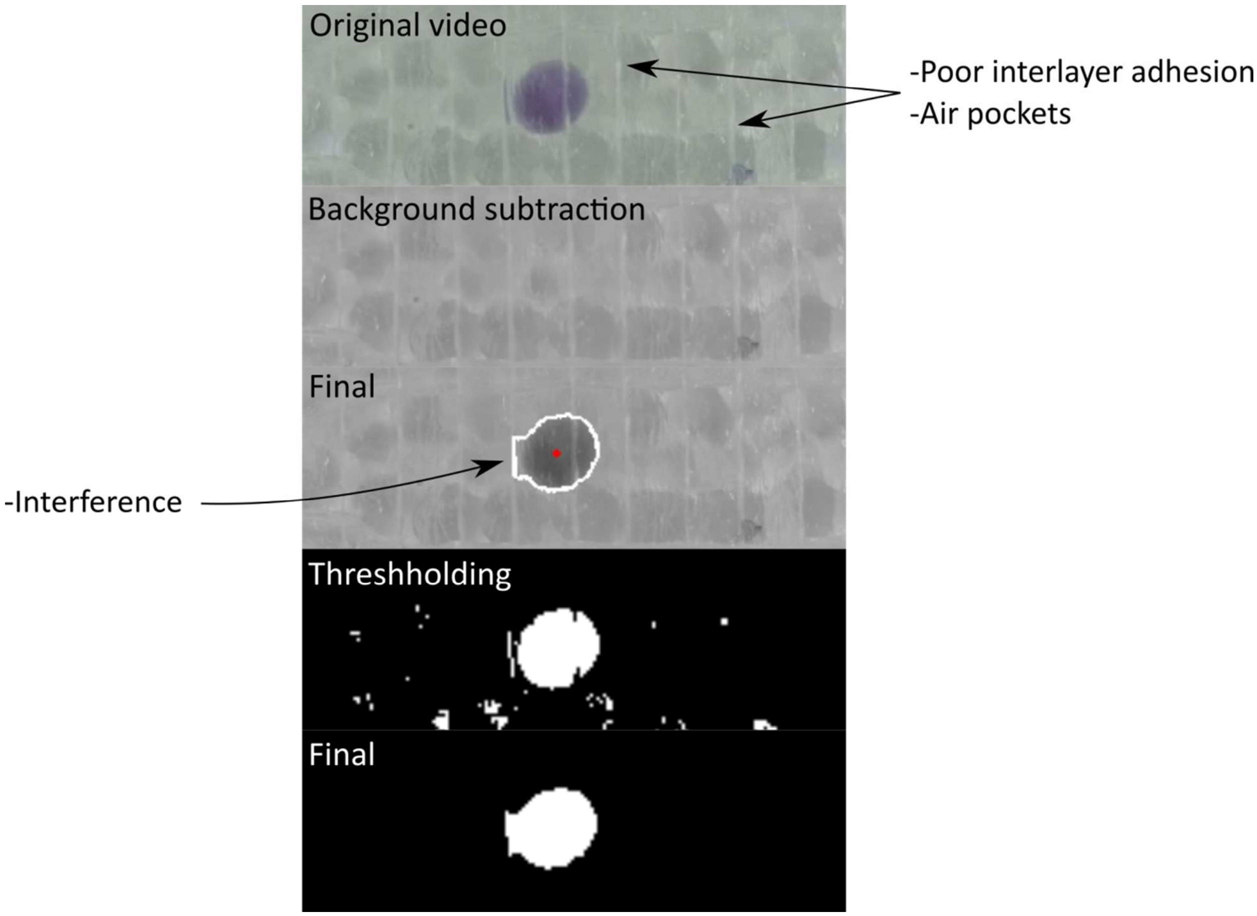

Figure S7. Traditional printing results in visible layer separation. Printing impurities and poor printing protocols with tradition approaches lead to clearly defined extruded filament separation. Upon image processing in the DMV software, interference is clearly visible.

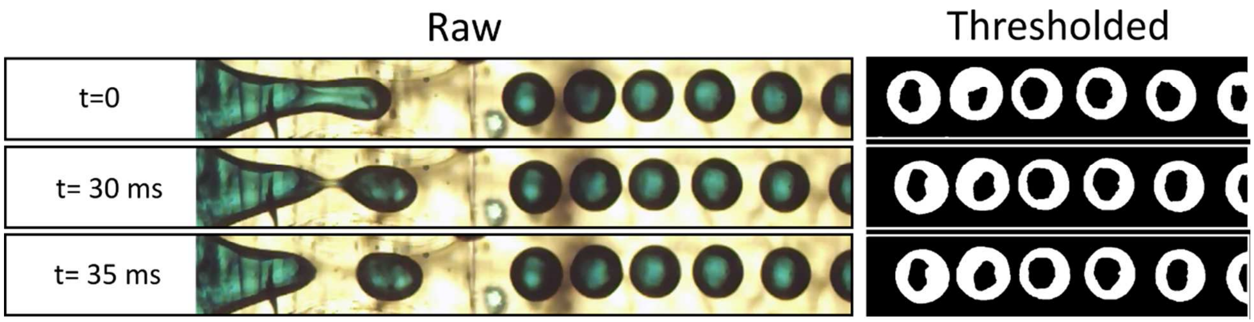

Figure S8. Water in oil droplet formation. High speed (2500 fps) tracking of droplet formation.

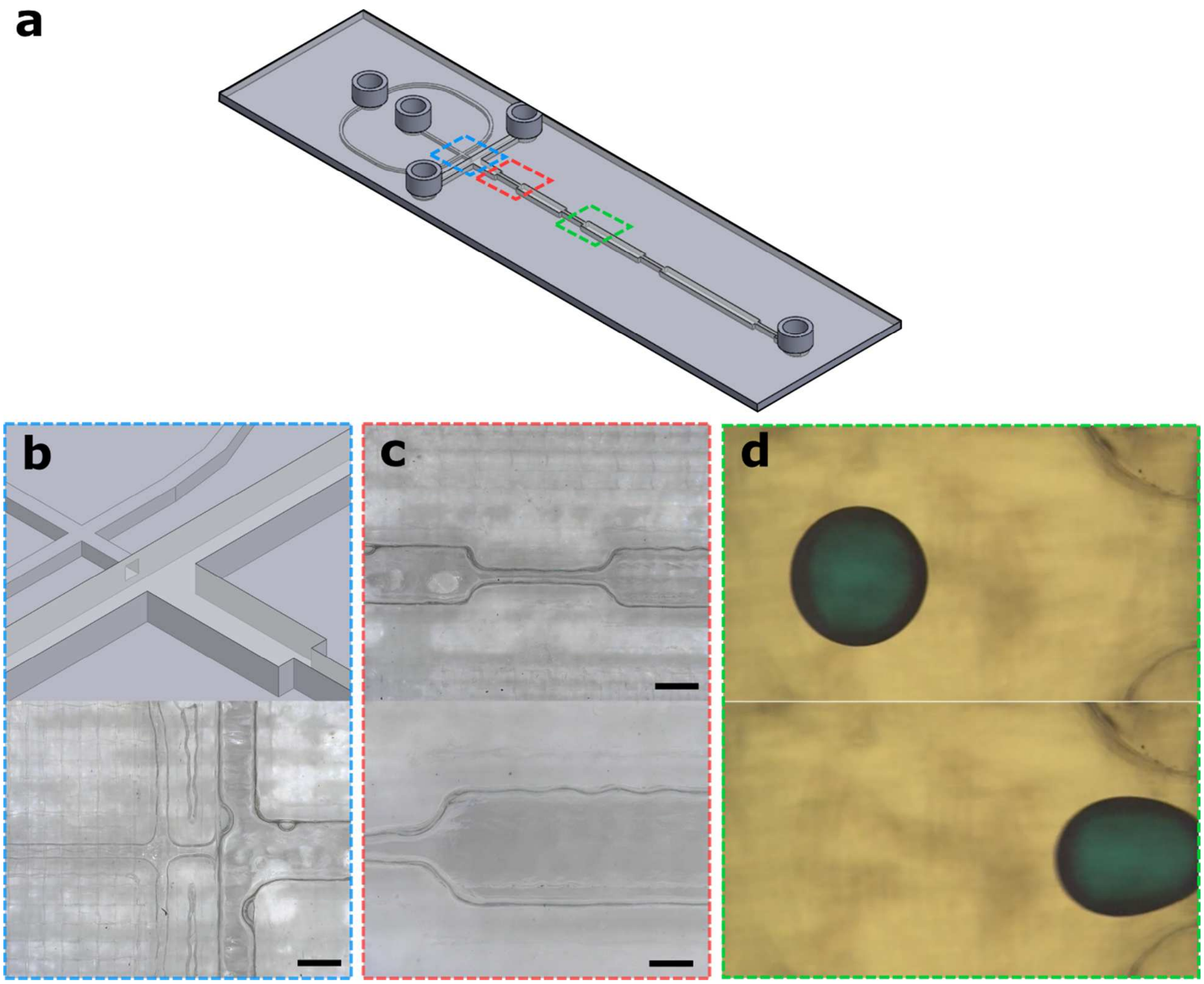

Figure S9. Imbedded channel. a, Schematic of a 3D droplet generator. b, CAD design of a 300 x 300 µm channel, imbedded 150 µm into the device. Optical micrograph of channels filled with air. Residual water can be seen inside the large channel. Scale bar, 1 mm. c, Constrictions used for deforming droplets. Scale bar, 1 (upper) and 0.5 mm (lower), respectively. d, High speed imaging of water droplets in oil. Droplet diameter ~ 500 µm.

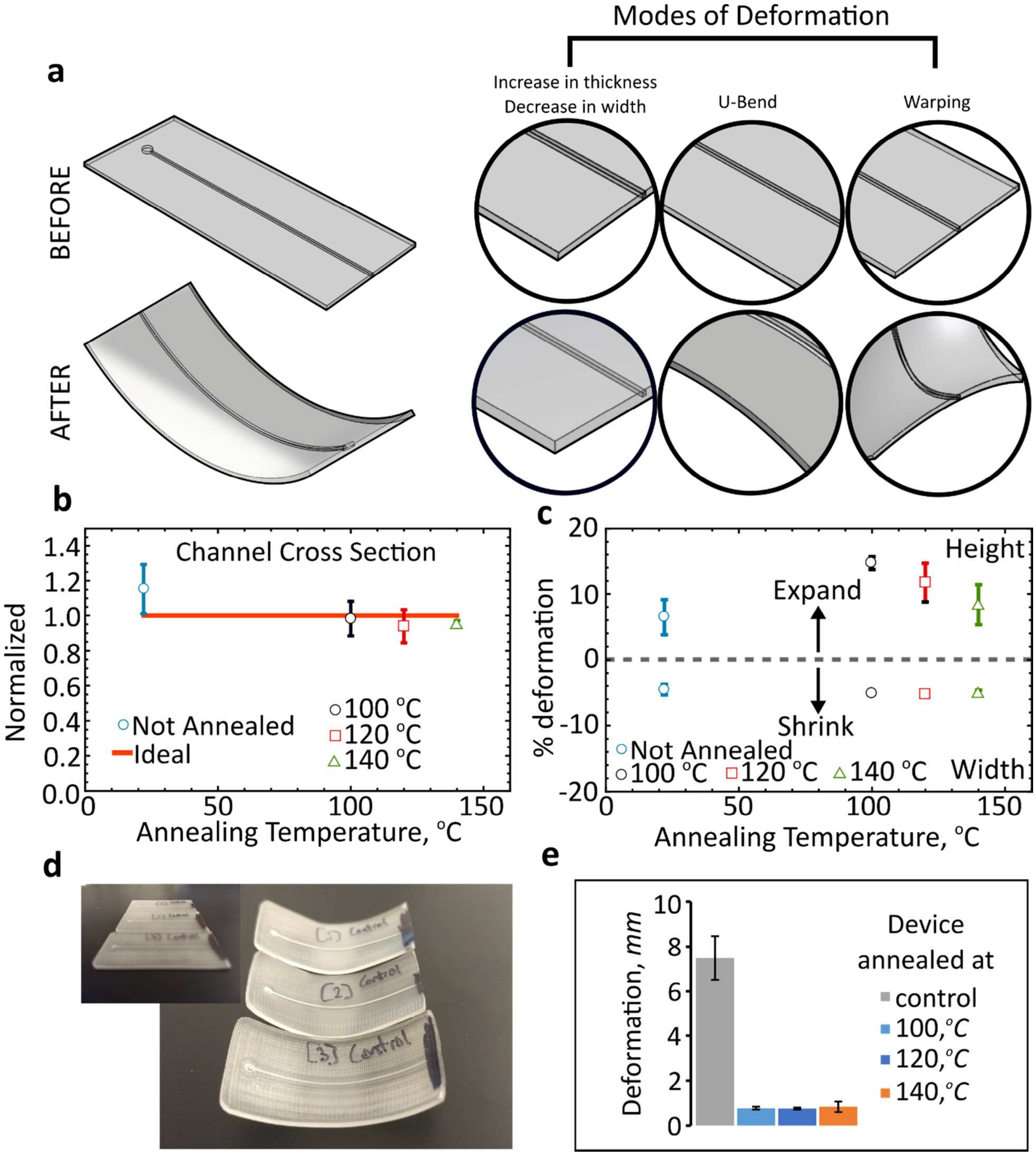

Figure S10. Annealing. a, CC-PLA modes of deformation before and after placement on to a hotplate at 95° C. b, Cross sections of un-annealed and annealed channels (n=3). c, Width and height changes of un-annealed and annealed devices (n=3). d, Deformation of un-annealed PLA devices when placed on a hotplate for 10 minutes at 95° C. Inset, before exposure. e, Impact of annealing on device deformation after placement on a hotplate at 95° C (n=3). Control is un-annealed PLA.

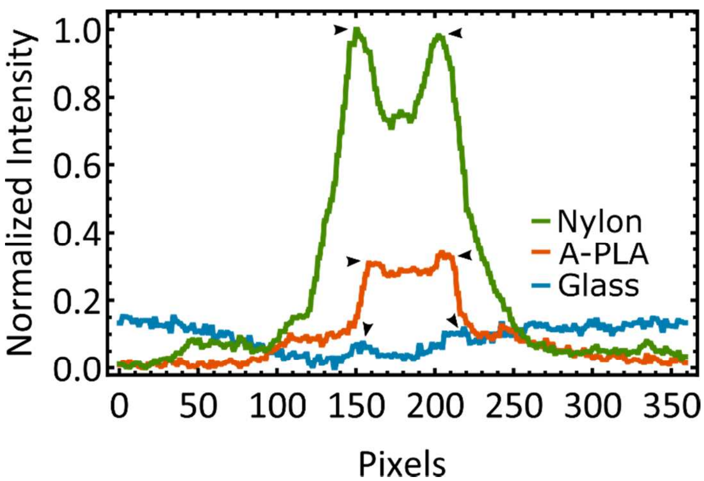

Figure S11. Autofluorescence of darkened devices. Autofluorescence of Nylon 680, Annealed PLA and Glass Slide-PDMS microfluidic channels. Arrows point to channel walls. Both 3D printed devices were darkened as per the protocol outlined above. A black tape was placed onto PDMS with autofluorescence visualized by looking through the glass slide.

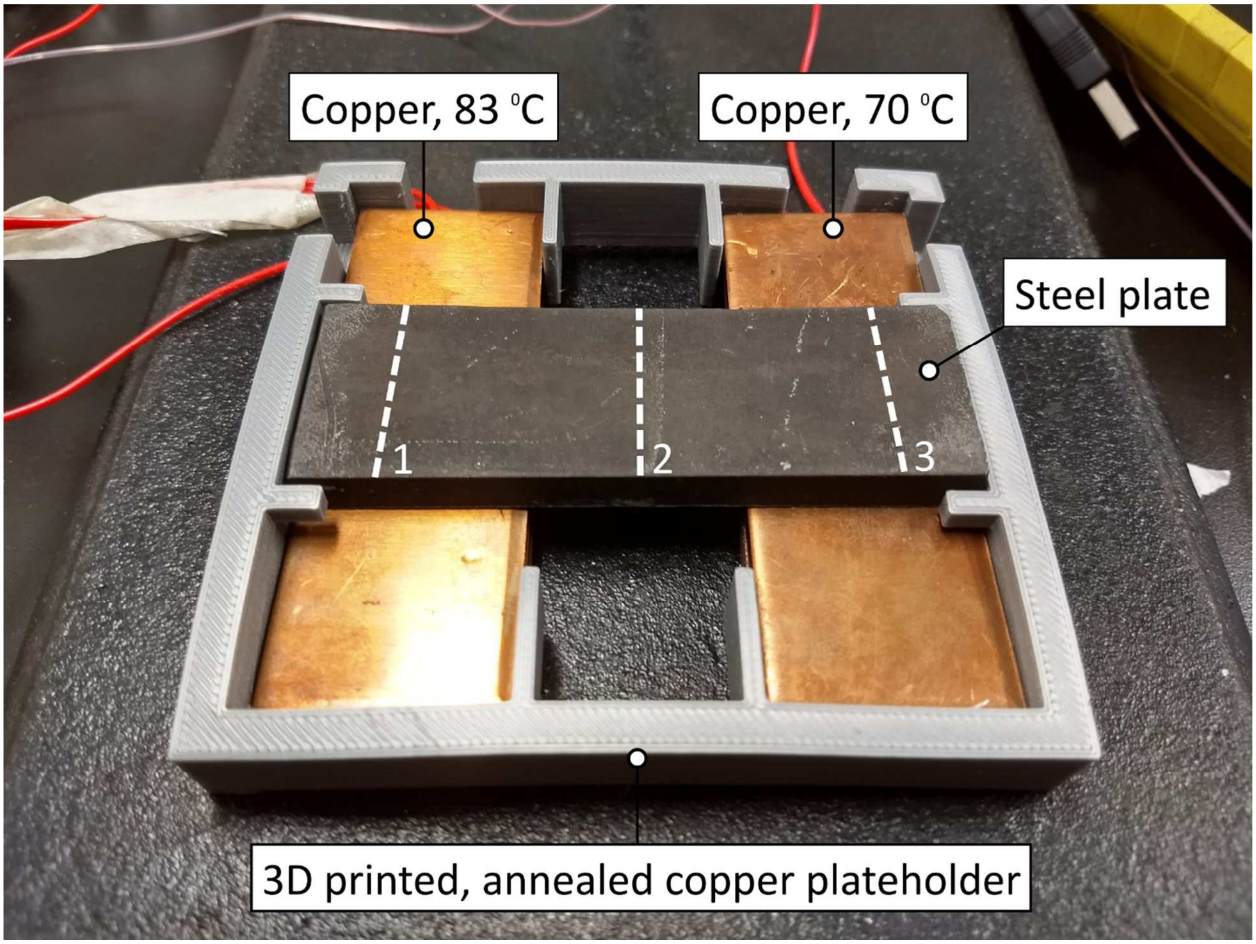

Figure S12. Experimental setup for thermal gradient generation. Copper blocks are housed within a 3D printed structure annealed at 150 ^{0}C. An enclosure housing LED lights is fitted on top preventing convective fluxes (not shown). Three thermocouples (not shown) affixed to the microfluidic device (not shown) at locations shown with the dotted lines, measure the temperature profile at any given time point.

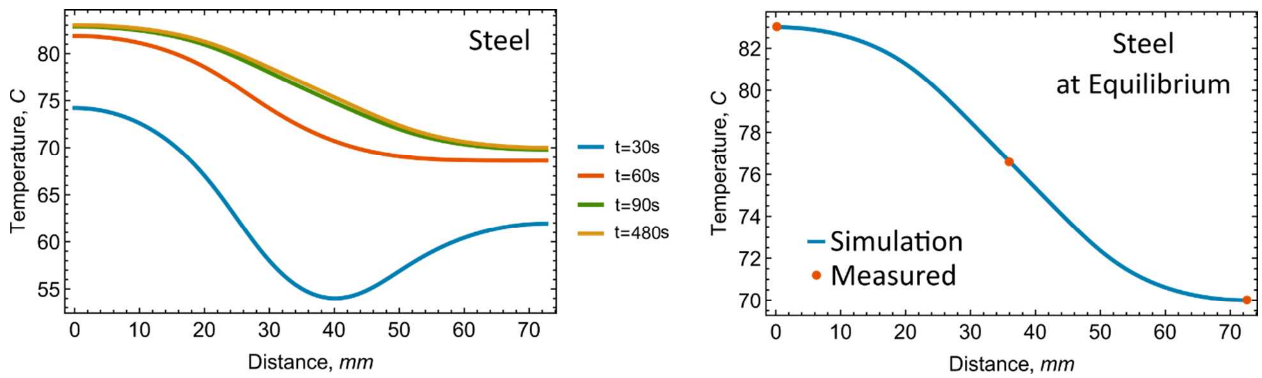

Figure S13. Temperature profiles for steel. Simulated temperature profiles for steel. Simulations suggest distinct regions where temperature is linear between the two copper plates. Temperature profiles at equilibrium compared to data measured from thermocouples show excellent agreement.

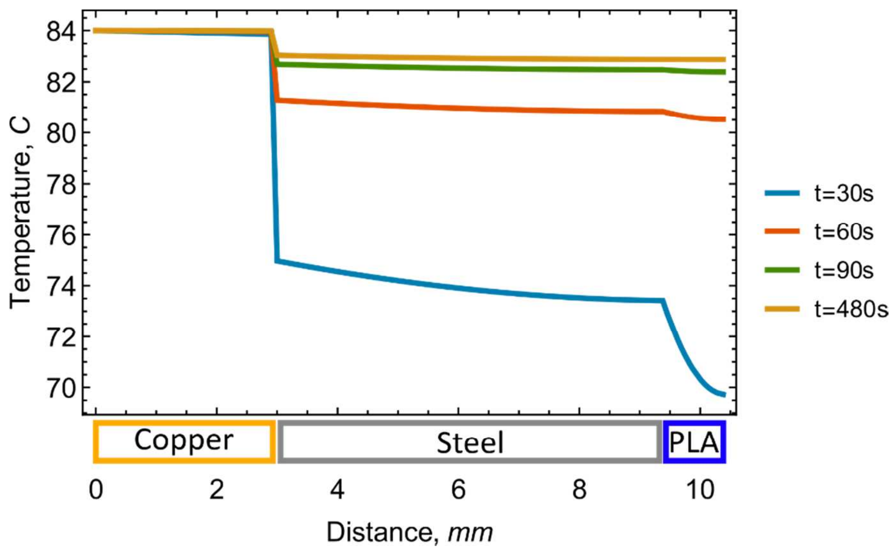

Figure S14. Temperature profile through the system. Due to the high thermal conductivity of steel and the relatively small thickness of the microfluidic device, the system is practically at equilibrium within 90 seconds.